-

Biogenic isoprenoid emissions under drought stress: Different responses for isoprene and terpenes

Boris Bonn[1], Ruth-Kristina Magh[1], Joseph Rombach[1], and Jürgen Kreuzwieser[1]

[1]Chair of Ecosystem Physiology/Chair of Tree Physiology, Faculty of Environment and Natural Resources, Albert-Ludwigs Universität, Georges-Köhler-Allee 053, D-79110 Freiburg i.Br., Germany

Correspondence: B. Bonn (boris.bonn@ctp.uni-freiburg.de)

Abstract. Emissions of volatile organic compounds (VOCs) by biogenic sources depend on different environmental conditions. Besides temperature and photosynthetic active radiation (PAR), the available soil water can be a major factor, controlling the emission flux. This factor is expected to become more important under future climate conditions including prolonged drying-wetting cycles. In this paper we use results of available studies on different tree types to set up a parameterization describing the influence of soil water availability (SWA) on different isoprenoid emission rates. Investigating SWA effects on isoprene (C_5H_8), mono- ($C_{10}H_{16}$) and sesquiterpene ($C_{15}H_{24}$) emissions separately, it is obvious that different plant processes seem to control the individual emission fluxes providing a measure of plants to react on stresses and to interact. The SWA impact on isoprene emissions is well described by a biological growth type curve, while the sum of monoterpenes displays a hydraulic conductivity pattern reflecting the plants stomata opening. However, emissions of individual monoterpene structures behave differently to the total sum, i.e. the emissions of some increase whereas ~~of~~ others decline at decreasing SWA. In addition to a rather similar behaviour as of monoterpene emissions, total sesquiterpene fluxes of species adapted to drought stress tend to reveal a rise close to the wilting point protecting against oxidative damages. Considering further VOCs too, the total sum of VOCs tends to increase at the start of severe drought conditions until resources decline. On the contrary contrary to declining soil water availability, OH and ozone reactivity enhance. Based on these observations a set of plant protection mechanism displays for drought stress and implies notable feedbacks on atmospheric processes such as ozone, aerosol particles and cloud properties. With progressing length of drought periods declining storage pools and plant structure effects yield different emission mixtures and strengths. This drought feedback effect is definitely worth consideration in climate feedback descriptions and for accurate climate predictions.

[RC2 1]
L.16

[RC2 2]
L.19

Copyright statement. TEXT

1 Introduction

Emissions of biogenic VOCs (E) are known to represent the largest contribution to global carbon flux besides carbon dioxide (CO_2) ~~and methane (CH_4)~~(IPCC, 2014; Niinemets et al., 2014; Holopainen et al., 2017). The emissions and the corresponding

[RC2 3]
L. 26

deposition rates (*exchange = emission+deposition*) are driven by temperature of vegetation (T_{veg}) and soil (T_{soil}), photosynthetic active radiation (*PAR*), ambient CO_2 mixing ratio, defense against herbivores (Manninen et al., 1998) and reactive air pollutants (Bourtsoukidis et al., 2012), plant-plant communication and competition, fire and drought (Lappalainen et al., 2009; Peñuelas et al., 2010; Guenther et al., 2012). The total amount of individual BVOC fluxes is linked to their production (*de*
5 *novo* synthesis or online) and storage (offline) capacities of individual plant types and species (Ghirardo et al., 2010) and is additionally affected by abiotic and biotic conditions. These include the temperatures of vegetation (T_{veg}) and soil (T_{soil}), photosynthetic active radiation (PAR), ambient CO_2 mixing ratio, defense against herbivores (Manninen et al., 1998) and reactive air pollutants (Bourtsoukidis et al., 2012), plant-plant communication and competition, fire and drought (Lappalainen et al., 2009; Peñuelas et al., 2010; Guenther et al., 2012). While BVOCs represent a large variability of different structures
10 and species (Goldstein and Galbally, 2007; Laothawornkitkul et al., 2009), it is commonly accepted that isoprene (C_5H_8) and monoterpenes ($C_{10}H_{16}$) display the majority (38-50% and 30%, respectively) of total BVOC exchange (1-1.3 Pg yr^{-1}) (Goldstein and Galbally, 2007; Guenther et al., 1995, 2012), if methane is excluded. The exchange *E* is commonly described by the exchange at standard conditions E_0 (*T* = 30 °C) and scaled by factors for individual driving forces such as temperature (*T*), light (*L*) (Guenther et al., 1995, 2006, 2012) or soil water content (*SWC*), here denoted as *SM* in the index in accordance with
15 the formulation of Guenther et al. (2006, 2012):

$$E \quad = \quad E_0 \cdot \gamma_T \cdot \gamma_L \cdot \gamma_{CO_2} \cdot \gamma_{SM} \tag{1}$$

Please find an overview of all the abbreviated terms and parameters in Table 1. Some of the scaling factors of driving forces (γ) for exchange are reasonably well-described regarding temperature and PAR, while other parameters like soil water availability (*SWA*) are mostly ignored due to a lack of understanding of influencing plant processes, although a simplified parameterisa-
20 tion exists (Guenther et al., 2012). This neglect is confronted with changing climate conditions such as warming of 0.15 °C ~~K~~/20 years (Schölzel and Hense, 2011) with predicted extending drought periods in Central European forest ecosystems such as the Black Forest in Southern Germany (Keuler et al., 2016; Kreienkamp et al., 2018). So far a single simplified formulation using a linear increase from no emission at the permanent wilting point (*PWP*) to maximum emission shortly above this point is commonly applied for different conditions. This is based on an experiment of poplar *Pegoraro2004a*, analyzing isoprene
25 only. The changing soil water conditions and the resulting change in BVOC exchange fluxes are expected to influence plant responses and protection capacities (Peñuelas et al., 2010; Rennenberg et al., 2006), the exchange following up ozone formation strength and further climate feedback processes (Bonn, 2014). In this study we aim at investigating the individual behaviour of isoprene, mono- (MT) and sesquiterpene (SQT) exchange fluxes and their correlation with *SWA* for available tree species to allow identification of processes controlling the emission. As European beech (*Fagus sylvatica*), which is *SWA* sensitive
30 (Gessler et al., 2007; Dalsgaard et al., 2011), is one of the most common tree species in Central Europe and of economic importance (Kändler and Cullmann, 2016), we will focus on the impact of the *SWA* effect on emissions.

[RC1 1]
L. 47

2 Materials and methods

2.1 Review of available studies and transfer between different water content parameters used

In order to develop an advanced description of the available water on BVOC exchange, available studies were collected, focusing on isoprenoid emissions in the context of different drought conditions. These studies include different tree types and several herbs predominantly under controlled conditions and for selected compounds or compound groups (Table 2).

2.2 Adapting available studies to a comparative scheme

2.2.1 Different conditions of individual studies

First, available studies on BVOC exchange for different tree species at different soil water conditions have been collected. It is important to note that these studies have been described in various ways using

(a) different soil water parameters (SWA, SWC_v and water matrix potential (Ψ_m)),

(b) different plant ages,

(c) different soil types,

(d) different lengths of investigation and time resolutions,

(e) with and without re-watering and

(f) different environments (laboratory, greenhouse and ambient).

The named different parameters complicate a direct comparison and include the assumption of an applicable transfer of laboratory or greenhouse experimental results with predominantly seedlings to ambient conditions, a transfer including notable challenges and questions as discussed e.g. by Niinemets (2010a).

2.2.2 Different parameters used for describing the effect of soil water

The plants access to soil water is best described by the accessible water SWA (index '%': fraction of accessible water, index 'v': volumetric amount) or by the suction pressure Ψ_m. Both parameters denote the soil water status and the ability of a plant to extract water from it (Blume et al., 2010). However, the easiest parameter to quantify soil water conditions by measurement continuously is volumetric SWC (SWC_v). Therefore, SWC_v has so far been used to estimate soil water effects on plants processes e.g. by Guenther et al. (2006, 2012). However, different soil types possess different PWP preventing water to be extracted by the plant below. Without the knowledge of the PWP of the soil investigated the information of SWC_v to describe the plant water access remains incomplete and makes different studies difficult to compare. Therefore, we focus on $SWA_\%$ as primary parameter for describing the soil water effect and provide a set of equations to transfer between the different quantities. This makes different amounts of soil water comparable for different soil conditions and furthermore allows an easy usage in

model studies that formerly used SWC_v (Guenther et al., 2006, 2012). To support this all parameterizations are stated by both, i.e. (a) by $SWA_\%$ and (b) by SWC_v. The *SWA* describes the amount of soil water above *PWP* (Ψ = -4.2 MPa) up to field capacity (amount of water held by the soil against gravity, *FK*, Ψ = -0.0063 MPa), and is called available or net field capacity (*nFK*) for the corresponding soil type, and which depends on the soil capacity to fix water (van Genuchten et al., 1980). During short terms *SWA* can exceed *nFK* (e.g. after an intense rain fall), but this excess water infiltrates the soil and is not available to the plant thereafter. A list of the different parameters used in the available literature is given and the transfer in between is assumed as (Blume et al., 2010):

$$SWA_\% = \frac{SWA_v}{nFK} = \frac{SWC_v - PWP}{nFK} \tag{2a}$$

$$SWA_v = SWC_v - PWP \tag{2b}$$

$$SWC_v = SWA_v + PWP \tag{2c}$$

$$= SWA_\% \cdot nFK + PWP \tag{2d}$$

$$nFK = \max(SWA_v) = FK - PWP \tag{2e}$$

$$FASW_\% = SWC_\% = \frac{SWC_v}{nFK + PWP} \tag{2f}$$

$FASW_\%$ and $SWC_\%$ abbreviate the volumetric soil water content relative to its maximum value (field capacity *FK*). Converting water or matrix potential ψ values is a function of the actual soil mixture of clay, sand and silt, i.e. the different corn size distributions/classes and the intercorn spaces available for water storage, which can be described by a water retention curve (van Genuchten diagram (van Genuchten et al., 1980), see e.g.Blume et al. (2010)):

$$SWA_\% = \frac{1}{nFK} \cdot ((SWC_{v,r} + \frac{SWC_{v,max} - SWC_{v,r}}{1 + (a \mid \Psi \mid \cdot 10^4)^{n^{1 - \frac{1}{n}}}} - PWP) \tag{3a}$$

$$SWC_v = SWC_{v,r} + \frac{SWC_{v,max} - SWC_{v,r}}{1 + (a \mid \psi \mid \cdot 10^4)^{n^{1 - \frac{1}{n}}}} \tag{3b}$$

$SWC_{v,r}$ is the residual SWC_v at completely air dried conditions, $SWC_{v,max}$ is the SWC_v at saturation, α the inverse of the air entry suction and *n* represents a measure of the pore-size distribution. Representative data for different soil textures can be found e.g. in Leij et al. (1996) and at http://soilphysics.okstate.edu/software/water/conductivity.html (access: 2019-01-17).

2.2.3 Different soil types, corresponding *PWPs* and *FKs*

PWP and *FK* values for different soil types were calculated from the articles information based on data summarized by Chen et al. (2001), and their common soil type classification. Different soil types, predominantly expressed by different corn sizes (corn diameter D_p) and pore space volume, available for soil water, can be classified according to the contribution of sand (0.002 mm $< D_p <$ 2 mm), silt (0.002 mm $< D_p <$ 0.050 mm) and clay ($D_p <$ 0.002 mm). Those mimic the potential of the soil texture to fix water, against which the suction pressure of plants needs to work for extracting soil water. This determines not only the *PWP* of the corresponding soil, i.e. the point at which a plant is unable to suck out any water of the soil pores, but also the maximum amount of water a soil can hold against gravity (*FK* or $SWC_{v,max}$). The individual studies published refer to

different soil types, *PWPs* and $SWC_{v,max}$ that need to be considered and included in a more general parameterization. Here, we use the contribution of individual soil types to the mixtures applied in the corresponding studies for calculating the *PWP* and the $SWC_{v,max}$. In order to make different soil types and conditions comparable, all soil water describing parameters were converted to $SWA_\%$ using *PWP* and *nFK*.

5   As this study is part of a beech – silver fir research project in Southwestern Germany most figures shown are displayed with two horizontal axes, (i) the reference $SWA_\%$ in percentage and (ii) an exemplary SWC_v describing the one at the projects field site in Freiamt, Black Forest, Southwestern Germany (Magh et al., 2018). This is representative for natural European beech soil common in Central Europe (Gessler et al., 2007) with a *PWP* of 4.7% and a *nFK* of 31.2%. In order to make results applicable to a wider range, any fitted equations take into account the soil properties and are provided for general conditions as

10   functions of (i) $SWA_\%$ (general reference) and of (ii) SWC_v (requires adaptation to local conditions).

2.3   Different fitting approaches and corresponding driving forces

The effect of soil moisture on the emission of BVOCs is described by Guenther et al. (2006, 2012) using three-step pattern: Assuming (1) no emission below the *PWP*, (2) a linear increase of emissions between *PWP* (γ_{SM} = 0) and *PWP*+4 vol% of SWC_v (γ_{SM} = 1) and (3) a soil moisture independent emission above. This empirical parameterization was based on isoprene

15   emission measurements of Canadian black poplar (*Populus deltoides*) at the Biosphere 2 facility (Pegoraro et al., 2004a). A different suggestion, exponential dependence of emission on SWC_v was published recently by Genard-Zielinski et al. (2018) for isoprene emissions too but for downy oak (*Quercus pubescens*) instead of black poplar.

For the overall soil moisture dependency of BVOC emissions at standard conditions (T = 30°C) several processes become important depending on the molecular size of the compound, its production and storage behavior as well as its water solubility.

20   (i) Stomata controlled effect: If the size of the BVOC molecule does not allow penetration of the leaf or needle surface layer the least barrier between plant and atmosphere are the stomata. Thus, the emission process is controlled by stomatal opening behaviour of the plant species (Simpson et al., 1985). Low $SWA_\%$ and SWC_v causes low Ψ - please note the negative scale, which triggers closure of stomata in order to increase the resistance for water molecules between leaf and atmosphere, helping to avoid loss of water by transpiration. Thus, γ_{SM} alters according to hydraulic conductivity pattern

25   (index '*h*') given as

$$\gamma_{SM,h} = a_h + \frac{b_h \cdot SWA_\%}{c_h + SWA_\%} = a_h + b_h \cdot \frac{(SWC_v - PWP)}{\frac{c_h}{nFK} + SWC_v - PWP}. \tag{4a}$$

The curve starts at ah, i.e. the residual emitted fraction at *PWP* and increases to unity as $SWA_\%$ reaches 100% at $SWC_{v,max}$ (*FK*). Both coefficients b_h and c_h determine the exact shape and slope of increase and are linked via

$$c_h = (b_h + SWC_v(PWP) - 1) \cdot (SWC_{v,max} - PWP). \tag{4b}$$

The shape is therefore different to the approach used in the MEGAN formulation (Guenther et al., 2006, 2012) as the effect sets in already below $SWC_{v,max}$.

5   (ii) Diffusion controlled effect: If the emission may take place at least partially through the *cuticula*, perhaps for smaller chemical species, loss of plant water will cause a bending of the tissue surface. This will increase the cell pressure and influence conditions and forces of contained smaller BVOCs leading to diffusion towards the ambient, i.e. emission. This process acts similar to biological growth processes and can be described by

$$
\begin{aligned}
\gamma_{SM,g} &= exp(-exp(b_g \cdot exp(1) \cdot (c_g - \frac{SWC_v - PWP}{nFK} + 1)) \\
&= exp(-exp(b_g \cdot exp(1) \cdot (c_g - SWA_\%) + 1)) \tag{5}
\end{aligned}
$$

Similar as above b_g as well as c_g represent curve shape parameters. The implicit γ_{SM} value at *PWP*, i.e. ag, is given by exp(-exp(b_g·exp(1)·(c_g)+1)).

(iii) Water solubility and transport effect: Further important processes as water dependent productivity or transport (e.g. via sap flow) will display either a linear behavior or a mixture of Eqs. 4a and 5. This depends on the limitations in the entire process chain from production, storage, potential transport and emission, which may be controlled by stomata opening or diffusion through the cuticula.

(iv) Plant defense or interaction effect: Finally, a rise of BVOC emissions shortly above the *PWP* is apparent in some MT but mainly SQT related studies. This may be explained by plant defensive strategies such as detoxification and reduction of radical oxidative species (ROS) species (Niinemets et al., 2014; Parveen et al., 2018; Piechowiak et al., 2019; Yalcinkaya et al., 2019), as most of these chemical species possess a high reactivity concerning ozone and radicals. The observations indicate an increase with decreasing $SWA_\%$ or SWC_v, until a rapid collapse close to *PWP*. We consider these observations to appear like a Gamma function type with a maximum near the *PWP*, i.e. $a \cdot (SWA_\% + b)^c \cdot$ exp(-$d \cdot (SWA_\% + b)$) with a set of parameters *a*, *b*, *c* and *d* characteristic for individual plant species. They may potentially reflect a species ability to respond to oxidative stress.

[RC1 2]
L.158ff

25 **2.4   Exemplary field studies: Application to ambient conditions**

2.4.1   Plant nursery, Freiburg

Eleven 8-10 years old *Fagus sylvatica* seedlings were studied in the plant nursery of the Chair of Ecosystem Physiology (48.014695° N, 7.832494° E) of the Albert Ludwigs Universität Freiburg with different soil water potentials, which were determined predawn and during daytime between July 19th and 31st 2018. Six trees served as control plants, which were

30 watered regularly, while rainwater was excluded by self-constructed roofs above the soil for the other five trees. The distance

between the edges of control and stressed group were approximately 10 m with 1 m distance between individual tree stems. Water was added by a watering pot by moderate flows to each of the trees in order to control the amount of water and to minimize the effects on neighbouring trees. Noteworthy, summer 2018 was extremely dry with less precipitation below 35 mm m^{-2} during June and July, which is only one third of the 30 year average (90.5±40.5 mm m^{-2}, Freiburg airport, distance: ca. 900 m NNW, German Weather Service, ftp://ftp-cdc.dwd.de/pub/CDC/observations_germany/climate/monthly/kl/) for those two months. Mean SWC_v of control and stressed beeches were approximated by two methods:, (i) the water potential of the experimental plants was determined with a Scholander pressure chamber (Scholander, 1966) at a cut branch predawn and around noon, and (ii) by SWC_v was estimated using measurements at a nearby field (ca. 600 m NW) with a similar soil structure (*VWC*, 10HS, Decagon, Washington, USA). BVOC emission with the method described by Haberstroh et al. (2018). For this purpose, BVOCs emitted from beech leaves were collected during daytime using air- sampling tubes filled with Tenax (Gerstel). Analysis occurred on GC-MS system (GC model 7890 B, GC System, MS: 5975 C VL MSD with triple-Axis Detector, Agilent Technologies, Waldbronn) equipped with a multipurpose sampler (MPS 2, Gerstel, Mülheim, Germany) (Magh et al., in prep.). More details on the analysis can be found here (Kleiber et al., 2017).

00 Based on the observed emission rates and corresponding forest air composition, relative changes in OH and ozone reactivity of the emission cocktail observed were derived as follows (Nölscher et al., 2014; Mogensen et al., 2015): The sum of the individual products of emission rates [molecules m^{-2} h^{-1}], and their corresponding reaction rate constants [cm^3 molecule^{-1} s^{-1}] was calculated and compared to the related sum of the undisturbed reference trees. This includes the knowledge of a large set of compound reaction rates of which some are not obtainable in the available literature. Those have been approximated using structure activity relationship (SAR) based algorithms developed by Neeb (2000) and McGillen et al. (2011). In order to do so, the molecule of interest was split in its functional groups and the respective coefficients used for the estimate. As this approach is relative (i.e. disturbed to undisturbed trees), effectsemissions of any vertical mixing is unimportant here, but will have to be considered for the detailed atmospheric impact on atmospheric chemistry, cloud properties and radiation (Seinfeld and Pandis, 2016) and its range. In this case, it is worth mentioning that forests extend usually to some tenths of kilometers in the Black Forest area and the area of emission can be easily traced back within the next kilometers in distance (unpublished data). This indicates the importance of BVOC emissions on the local atmospheric chemistry.

2.4.2 Black forest conditions at Freiamt

SWC_v values were measured at five different depths (5, 10, 25, 50 and 75 cm) with a time resolution of 2 h. Sensors were placed at different locations to test the heterogeneity, especially beneath different tree types, i.e. European beech (*Fagus sylvatica*) and Silver fir (*Abies alba*) and in between. For further information on measurements see Magh et al. (in prep.). In order to approximate ambient SWC_v effects on isoprene and terpene emissions, Eqs. 1, 4a, 5 and 10b have been applied to meteorological measurements nearby and SWC_v.

3 Results

As indicated in section 2.3 we standardized and tested the influence of available soil water on emission rates of isoprene (E_{isop}), MT (E_{MT}) and SQT (E_{SQT}) using different hypotheses, a) a stepwise effect (Guenther et al., 2006), b) a growth rate like behavior (Eq. 5), ca) a hydraulic conductivity pattern (Eqs. 4a and b) as well as d) a stress defense response of $SWA_\%$ (lower x-axis) and for comparison the SWC_v for a selected condition (upper horizontal axis).

[RC1 6]
L.203

3.1 Isoprene

Most studies on plant BVOC emissions affected by limited amounts of soil water investigated isoprene. A summary plot of individual studies rescaled to comparable conditions is provided in Fig. 1. In here the corresponding $SWA_\%$ conditions are plotted vs. γ_{SM}. A secondary horizontal axis on the top of Fig. 1 displays typical SWC_v representative for Black Forest conditions at the Freiamt site (*PWP* = 4.7, *nFK* = 31.2%, soil: loamy sand; Magh et al. (2018)). These conditions are similar to what has been found for European beech forest conditions elsewhere (Dalsgaard et al., 2011). Values of γ_{SM} displayed were obtained from measured emission rates (Pegoraro et al., 2004a, b; Brilli et al., 2007; Fortunati et al., 2008; Bourtsoukidis et al., 2014) and were divided by either (a) the corresponding measurements at well-watered standard conditions or (b) by literature values for the individual plant species. More information on the individual datasets and studies is provided in Table 2. Some values such as *PWP* and *nFK* are assumed according to the information provided by the authors of the corresponding studies. The figure clearly indicates that most of the studies focused on a specific smaller frame of the entire $SWA_\%$ range and only a single value has been measured below the *PWP*. This smaller range tended to yield a simplified description as for example the dataset of Pegoraro et al. (2004a), which was used by Guenther et al. (2006, 2012)(residual standard error (*RSE*) = 0.163, r^2 = 0.65). Testing different models for the dominating processes, the biological growth curve was found to fit the available datasets best (*RSE* = 0.06).

$$\gamma_{SM}(isop, fit, growth) = exp(-exp((0.056 \pm 0.001) \cdot exp(1) \cdot (-(2.3 \pm 1.5) - SWA_\%) + 1)) \tag{6a}$$

$$= exp(-exp(\frac{(0.056 \pm 0.001)}{nFK} \cdot exp(1) \cdot (-(5.4 \pm 3.5) - (SWC_v - PWP)) + 1)) \tag{6b}$$

Apparently, limited soil water access seems to influence isoprene emissions predominantly by growth stress and less by stomatal opening, although growth stress and stomatal opening share similar features in a plot like Fig. 1 and only the entire $SWA_\%$ range allows discrimination between the two. Isoprene may diffuse out of the plant because of its smaller molecular size. Thus, a nearly closed stomata may not protect the plant from the release of isoprene because of enhanced cellular concentrations at reduced stomatal opening (Simpson et al., 1985; Fall and Monson, 1992).

3.2 Monoterpenes

The situation for monoterpenes (MT) is more complex as different MT isomers display a different behaviour with decreasing $SWA_\%$ (and SWC_v, Fig. 2). For example, in the case of European beech (*Faguchs sylvaticasylvestris*) the dominant MT sabinene (Moukhtar et al., 2006) declines drastically with reduced water availability, but limonene to a smaller extentd, whereas

[RC2 10]
L.230

trans-β-ocimene stays constant within the uncertainty limit (Rombach, 2018). Lüpke et al. (2017a) report declines in α- and β-pinene, limonene and myrcene emissions in response to increasing drought stress on Scots pine (*Pinus sylvestris*), while Δ^3-carene emissions remained unaffected. An isotopic labeling test displayed a tendency of negatively influenced *de novo* production and contribution with declining SWC_v and thus $SWA_\%$, while emission of stored monoterpenes was less affected.

5 This may explain the overall behavior of MT emission and propose the storage pools to determine the total amount of emissions. If so, any damage to cell walls or other plant structure elements, and extensive drought length will cause a) a significant decline in total emissions beyond the drought period on the long term, and b) the ability of the plant structure to recover, to form and store new MT as before. Individual MT structure behaviour however will depend on their detailed production pathway and storage location within the plant. Ormeño et al. (2007) describe an increase of MT emissions by rosemary (*Rosmarinus*

10 *officialis*) at reduced soil water supply under Mediterranean conditions. The individual contribution of different structures even display a further process to be noted: The relative contribution of α-pinene increased at reduction of SWC_v from 21% to *PWP* and dropping thereafter similar to a stress response until cell damage was observed. A secondary contribution increase at very low SWC_v values observed for Sweet chestnut (*Castanea sativa*; Lüpke et al. (2017b)) may result from changes in very small emission amounts and appears as large uncertainty range awaiting further investigation. The remaining emission flux below

15 *PWP* may result from *de novo* production or from different storage locations, which are still functioning properly. Emissions of sabinene behave in a very similar way to the ones of α-pinene, while the fluxes of myrcene transiently increase around *PWP*. The opposite is true for cineole contribution that drastically declines with reducing SWC_v and displays only at notable soil water presence. MT emissions of Aleppo pine (*Pinus halepensis*) display a pattern insignificantly influenced by γ_{SM} vs. SWC_v for α-pinene, Δ^3-carene and linalool, while β-pinene and myrcene tend to increase. Total kermes oak (*Quercus*

20 *coccifera*) emissions of MT do not change significantly as well, but the contribution of α-pinene to total MT emissions enhances continuously even beyond the *PWP*. Therefore, the effect of individual MT structures depends on production rate as well as on storage pools and locations, which differ for different plant species. By changing the MT mixture plants may adapt to different stress conditions for improved defense (more details in section 3.5). However, the total MT emission effect of limited soil moisture seems to be more general.

25 A representative plot indicating the influence of $SWA_\%$ on total MT emissions is shown in Fig. 2. The set-up is identical to Fig. 1 for isoprene, i.e. the different studies included are marked with different symbols and colours. Lighter colours represent conditions after rewetting if performed as for instance for Scots pine (*Pinus sylvestris*) (Lüpke et al., 2017a). Lighter points indicate a severe plant structure damage and not entirely recovered plants reaching a lower emission intensity as has been observed in several studies. Excluding those and assuming a soil water supply above *PWP*, different fits can be applied to

30 the entire dataset. While all data scatter notably, the best performance is obtained with the hydraulic conductivity approach (residual standard error (*RSE*) = 0.02), which is stomata opening controlled. Eventually the biological growth fit (*RSE* = 0.14) works appropriately if the smallest values are neglected. However, the three-step approach by Guenther et al. (2006, 2012) used for isoprene fails (*RSE* = 0.69) to appropriately describe the observations. Due to different abilities to store MT as commonly

[RC2 1

L.263

denoted as offline and only temperature driven emissions the lower end of the fit displays a notable variance.

$$\gamma_{SM}(MT, fit, hyd.) = (0.22 \pm 0.05) + (0.78 \pm 0.05) \cdot ((1.3 \pm 0.1) \cdot \frac{SWA_{\%}}{(33 \pm 3)\% + SWA_{\%}} \tag{7a}$$

$$= (0.22 \pm 0.05) + (0.78 \pm 0.05) \cdot ((1.3 \pm 0.1) \cdot \frac{(SWC_v - PWP))}{\frac{(33 \pm 3)\%}{nFK} + (SWC_v - PWP)} \tag{7b}$$

$$\gamma_{SM}(MT, fit, growth) = exp(-exp((0.019 \pm 0.004) \cdot exp(1) \cdot (-(5.0 \pm 1.2) - SWA_{\%}) + 1)) \tag{8a}$$

$$= exp(-exp(\frac{(0.019 \pm 0.004)}{nFK} \cdot exp(1) \cdot (-(5.0 \pm 1.2) - (SWC_v - PWP)) + 1)) \tag{8b}$$

Note, the $SWA_{\%}$ effect is less punctual at a specific $SWA_{\%}$ than in the case of isoprene and the specific slope is soil, i.e. nFK and PWP, dependent. The decline in emission strength gets already larger than 5% by $70 \pm 5\%$ of the accessible $SWA_{\%}$, depending on the fitting model chosen, not at about 6 ± 2 in the case of isoprene as similarly found by Guenther et al. (2012).

10 However, the lower edge of the fitting is different but important especially for arid regions and their corresponding emissions. On average about $22\pm5\%$ of the total MT emissions remain unaffected by soil water content (at *PWP*).

3.3 Sesquiterpenes

Based on the molecular properties such as saturation vapour pressure (Seinfeld and Pandis, 2016), water solubility (Sander, 2015), and capability to be stored (Kosina et al., 2012), the effect of $SWA_{\%}$ on the emissions of sesquiterpenes (SQT, $C_{15}H_{24}$)

15 (Duhl et al., 2008) behaves the same way as seen for MT (Fig. 3), i.e. emissions are predominantly affected by plant hydraulic conductivity (*RSE* = 0.153), which is controlled by stomatal opening. Applying the same approach as done for monoterpenes above, yields the following results for the soil moisture effect on total sesquiterpene emission rates γ_{SM}(SQT):

$$\gamma_{SM}(SQT, fit, hyd.) = (0.22 \pm 0.04) + (0.78 \pm 0.04) \cdot \frac{(1.75 \pm 0.5) \cdot SWA_{\%}}{(81 \pm 57)\% + SWA_{\%}} \tag{9a}$$

$$= (0.22 \pm 0.05) + (0.78 \pm 0.05) \cdot (1.75 \pm 0.5) \cdot \frac{(SWC_v - PWP)}{\frac{(81 \pm 57)\%}{nFK} + (SWC_v - PWP)} \tag{9b}$$

20 The onset of emission reduction with decreasing $SWA_{\%}$ sets in even earlier compared to MTs (Rombach, 2018), as indicated by the different slopes in Fig. 3 and in Eqs. (9a and 9b). However, individual structures reveal a large scattering at lower $SWA_{\%}$ and thus SWC_v values (<10%) that is supposed to result from plant defensive strategies/mechanisms and perhaps from damage to cell walls and membranes.

3.4 Potential additional effects near the wilting point for terpenes

25 For some plant species e.g. *Cistus albidus* and rosemary (*Rosmarinus officialis*), the effects of limited access to soil water on MT and SQT emission fluxes reveal a second maximum other than the one at γ_{SM} = 1, appearing near the *PWP* (Figs. 4, S3-S8). Highly temperature- and drought stress adapted species with the ability of to produce large amounts of terpenoids (e.g. *Cistus ladanifer* (Haberstroh et al., 2018) and *Rosmarinus officialis* (Ormeño et al., 2007)) display a second maximum close

to *PWP* not only for some of the MT (*Cistus ladanifer*: d-limonene, myrcene and trans-β-ocimene (Haberstroh et al., 2018); *Rosmarinus off.*: α-pinene and β-myrcene (Ormeño et al., 2007)) but also for some of the SQT and diterpenes (DT)(*Cistus ladanifer*: α-cubebene, α-farnesene, ent-16-kaurene and β-chamigrene (Haberstroh et al., 2018); *Rosmarinus off.*: Δ-cardinene and α-zingiberene (Ormeño et al., 2007), Fig. 4) and even the sum of all. This is apparent for instance in the studies of Ormeño

et al. (2007) and Haberstroh et al. (2018) of a broader range of plant species. As can be seen in Figs. S3-S8 (supporting online information), there is a statistically significant difference between individual chemical structures for different plant species, indicating a specifically adopted plant species. If those plots are investigated in more detail it is apparent that for example the monoterpene α-pinene increases with decreasing $SWA_\%$ for *Rosmarinus officalis* (S6) and *Quercus coccifera* (S5), but persists for *Pinus halepensis* (S4) (Ormeño et al., 2007). The emission of the monoterpene β-pinene is declining for *Cistus albidus* (S3), stays put for *Rosmarinus officialis* (S6) and enhances for *Pinus halepensis* and *Quercus coccifera*. Similar observations can be made for SQT emissions with *SM* values near the *PWP*: Δ-cadinene emissions increase with decreasing *SM*, while α-zingiberene emission decline for *Rosmarinus officialis*. Haberstroh et al. (2018) monitored decreasing emission fluxes for all the individual chemical SQT structures for *Cistus ladanifer* and *Quercus robur* in a very narrow *SM* range ($SWA_\%$ = ca. 0-6 %). This is opposite to the behaviour of *Cistus albidus* (Ormeño et al., 2007). Δ-germacrene emissions tend to increase near the *PWP* for *Cistus albidus*, *Quercus coccifera* and *Rosmarinus officialis* (Figs. S3, S5 and S6).

The enhanced emitted chemical species are known to possess a substantially higher reactivity with respect to ozone, which is usually elevated at drier conditions on longer time scales because of enhanced production rates and accumulation (see section 3.7). For example α-pinene possesses an O$_3$ reaction rate constant (k_{O3}) of 8.66×10^{-17} cm^{-3} molecule^{-1} s^{-1}, compared to the ones of β-pinene and Δ^3-carene of 1.5×10^{-17} and 3.7×10^{-17} cm^3 molecule^{-1} h^{-1}, respectively (Atkinson et al., 1990). With respect to the OH reaction, β-pinene reacts faster~~d~~ (k_{OH} = 7.89×10^{-11} cm^3 molecule^{-1} h^{-1}), followed by α-pinene and Δ^3-carene with corresponding rate constants $k_O H$ of 5.37×10^{-11} and 0.88×10^{-11} cm^3 molecule^{-1} h^{-1}, (Atkinson and Arey, 2003). This can be extended for other monoterpenes if more data especially on d-limonene, terpinolene and other very reactive MTs would be available. However, the number of data for individual species is quite limited and depends on different plant ages, which does not allow deriving a trustworthy equation at this stage. Sometimes the number of data points is equal to the number of parameters to constrain. The situation looks similar for *SM* effects on SQT emission rates. Consider e.g. the bottom plot for SQT in Fig. 4, displaying allo-aromadendrene, Δ-germacrene, Δ-cadinene and α-zingiberene. Reaction rate constants k_{O3} with respect to ozone are 6.5×10^{-16}, unknown, 3.2×10^{-16} and unknown, respectively. The corresponding k_{OH} for OH reactions are 1.5×10^{-10} cm^3 molecule^{-1} h^{-1} for aromadendrene, with the further ones not accessible based on experiments. However, structure-activity relationships such as US EPA (2018), indicate constants of ca 10^{-10} cm^3 molecule^{-1} h^{-1}. Thus, we assume this secondary maximum to occur as detoxification and defensive strategy of the plants (Kaurinovic et al., 2010; Höferl et al., 2015). Because of notable variations in measurements this effect is not significant for all the Mediterranean species, but for the *Cistus ladanifer* and *Rosmarinus officialis* measurements. To incorporate this feature near the *PWP* exemplarily, which tends to be linked to higher ozone concentrations, this secondary maximum can be taken into account using a Gamma function

term added to the hydraulic conductivity curve ($RSE = 0.147$) in Eqs. 10a and 10b:

$$\gamma_{SM}(SQT, fit, hyd.)^* = (0.22 \pm 0.04) + (0.78 \pm 0.04) \cdot ((1.75 \pm 0.5) \cdot \frac{SWA_\%}{(81 \pm 57)\% + SWA_\%}$$
$$+ a \cdot (SWA_\% + b)^c \cdot exp(-d \cdot (SWA_\% + b)) \tag{10a}$$

$$\gamma_{SM}(SQT, fit, hyd.)^* = (0.22 \pm 0.04) + (0.78 \pm 0.04) \cdot ((1.75 \pm 0.5) \cdot \frac{(SWC_v - PWP)}{\frac{(81 \pm 57)\%}{nFK} + (SWC_v - PWP)}$$
$$+ a \cdot (\frac{SWC_v - PWP}{nFK} + b)^c \cdot exp(-d \cdot (\frac{SWC_v - PWP}{nFK} + b)) \tag{10b}$$

a, b, c and d state parameters for the individual response of plant species to severe drought stress Gamma function) and they need to be adapted to the exact plant or ecosystems response studied on the local scale. An example is shown by the green line in Fig. 3 (applied parameters in here for *Cistus ladanifer* and *Rosmarinus officialis*: $a = 0.4$, $b = 1.57$, $c = 0.6$, $d = 1$). It is of interest that different structures seem to behave differently according to their historical stress adaptation as presented by Fortunati et al. (2008) and Lüpke et al. (2016). On the contrary to the hydraulic conductivity related description, the stepwise approach (Guenther et al., 2006) applied for isoprene fails in reproducing the declining pattern accurately ($RSE = 0.895$).

[RC2 14

L.311

3.5 Further BVOC emission rates

In addition to isoprene, MT and SQT, other VOCs are released by plants in notable amounts, but for which the impact of soil moisture is even less studied. Because of the huge number of different oxidized species and related publications including those within the parameterization would extend this study largely. A snapshot of individual correlation coefficients of different compound groups and species can be seen in Figure S1. A non-negligible role of those larger VOCs seems plausible, either via formation pathway or oxidation processes within the plant. Those species supply further molecules that can buffer oxidative stresses onto the plants internal processes. Additionally, they have substantial implications on especially the OH reactivity (Atkinson et al., 1990; Atkinson and Arey, 2003; Neeb, 2000; Müenz, 2010; Seinfeld and Pandis, 2016; US EPA, 2018). Overall, there is a tendency (Rombach, 2018) for an increased total BVOC emission under drought stressed conditions, but there is a large scatter of individual species reaction. However, the implications for OH reactivity and thus atmospheric chemistry are of relevance as this parameter describes the plants ability to still counteract oxidative damages by BVOC emissions.

[RC2 1

L. 344

3.6 Effects on reactivity

As chemical oxidation and ROS cause substantial damage to plants (Loreto and Velikova, 2001; Oikeawa and Lerdau, 2013) especially at stressed conditions such as at warm and dry conditions, any strategy of plants to counteract or detoxify will be beneficial for survival and plant competition. An indication for this may be seen in the local emission increase of SQT near *PWP* for some plant species. Saunier et al. (2017) found a stable ratio of catabolic to anabolic BVOC emissions, i.e. emission fluxes related to oxidation stress and to non-oxidative stress production, respectively, during recurring drought periods for downy oak (*Quercus pubescens*) at Mediterranean conditions. This is different for different plant types and their adaptation to stress conditions (Niinemets, 2010a, b), i.e. the need to compensate oxidative stress for survival. Looking at the pattern of absolute

and relative MT and SQT emissions with declining $SWA_\%$ values, it becomes obvious that more reactive structures tend to increase until plant cell damages occur (Ormeño et al., 2007; Bourtsoukidis et al., 2012; Nölscher et al., 2016). Especially SQT emissions displaying this transient peak around *PWP* cause a remarkable change. For example reducing the SWC_v for European beech by approximately 3 vol% close to *PWP* increases the total emission of SQTs by 170%. The individual SQT species, however, show different patterns (Table 3). While emission of junipene declines (-50%), the one of longifolene stays constant within the uncertainty limits and the corresponding fluxes of isolongifolene, α-bergamotene and α-farnesene increase drastically (+50%, +500% and +700%). Other VOCs analyzed (total: 81 VOCs; Rombach (2018)) operate in various ways: sabinene emission nearly vanishes at *PWP*. On the contrary, emission of α-terpineol increased. Overall, the total emissions of VOCs and C increased tentatively (Fig. 5). This caused total OH reactivity and especially ozone reactivity to tentatively enhance (OH: $+39^{+88}_{-46}\%$ and O$_3$: $+131^{+265}_{-104}\%$) at a SWC_v change of approximately 3 vol%. In this way the total amount, the changing composition and reactivity provide a tool for plants in this example for European beech to counteract oxidative stress and damages. The median change in OH reactivity corresponds nicely to the increase in total carbon emitted, as most organic species react with OH. However, the change in ozone reactivity is primarily related to the changes in individual SQT emissions. The large uncertainty in this context results from partially unknown reaction rate constants estimated either from similarity or from structure activity relationships (SAR) (Neeb, 2000; McGillen et al., 2011). Since the storage pools especially of larger terpenes will be depleted with prolonged duration of drought, this effect will weaken over time.

3.7   Application to atmospheric conditions: Ambient SWC_v and its effect on emission rates at the reference site

In order to test the impact of the described effects of $SWA_\%$ and thus SWC_v on isoprenoid emissions we apply the following emission flux parameterizations for isoprenoids from European beech and silver fir, which were quantified in earlier studies in this region excluding the $SWA_\%$ effect (Moukhtar et al., 2005, 2006; Šimpraga et al., 2011; Bonn et al., 2017):

$$E_{isop}(Fs) = 0\,\mu g\,g(dw)^{-1}h^{-1} \cdot C_T \cdot C_L \tag{11a}$$

$$E_{MT}(Fs) = 43.5\,\mu g\,g(dw)^{-1}h^{-1} \cdot C_T \cdot C_L \tag{11b}$$

$$E_{SQT}(Fs) = 0.04\,\mu g\,g(dw)^{-1}h^{-1} \cdot exp(0.11°C^{-1} \cdot (T_L - 30°C)) \tag{11c}$$

$$E_{isop}(Aa) = 0.038\,\mu g\,g(dw)^{-1}h^{-1} \cdot C_T \cdot C_L \tag{11d}$$

$$E_{MT}(Aa) = 28.8\,\mu g\,g(dw)^{-1}h^{-1} \cdot (0.71 \cdot exp(0.14°C^{-1} \cdot (T_L - 30°C))) + 0.29 \cdot C_T \cdot C_L) \tag{11e}$$

$$E_{SQT}(Aa) = 0.13\,\mu g\,g(dw)^{-1}h^{-1} \cdot exp(0.04°C^{-1} \cdot (T_L - 30°C))) \tag{11f}$$

SM effects on specific emission rates have been calculated by including and excluding the individual γ_{SM} factors as multiplicand on the results. In Eqs. 11a-f C_T and C_L abbreviate the temperature and light scaling factors of Guenther et al. (1995), as well as T_L the temperature of the needle or leaf surface in °C.

The base effect of soil water on isoprenoid emission rates can be exemplarily shown assuming a temperature of 30°C, i.e. standard conditions (see Fig. S2 in supporting online information). The available soil water for a plant has different impacts at distinct $SWA_\%$ values. At $SWA_\%$ (i.e. SWC_v (Freiamt) = 20%) of 35% isoprene emission rates display no decline, while the

corresponding ones of MT and SQT reduce by 15 and 25%, respectively. Assuming an $SWA_\%$ of 10% ($SWC_v = 10\%$ with a *PWP* of 4.8% at Freiamt), isoprene, MT and SQT emission rates represent only 95, 50 and 40% of the standard rates. Therefore, the amount of soil water has strongest effects on the larger terpenes shrinking with molecular size. Isoprene emissions will stay unaffected longer than MT and will keep ozone production high if isoprene is the dominant class of isoprenoids released by the ecosystems in the nearby region. Depending on the tree specific emission – i.e. on- and offline including temperature effects – different locations of emission optima or maxima are found (Fig. 6). The predominantly *de novo* emitting European beech will emit highest close to 30°C, while the maxima of silver fir emission rates are shifted to larger temperatures. Similarly the effects of changing *SM* will occur at the very same temperatures.

The overall impact of variable *SM* pattern on isoprenoid emissions was investigated using an exemplary SWC_v data at five different depths. Those measurements were located within the reference stand of a European beech (*Fagus sylvatica*, Fs) and silver fir (*Abies alba*, Aa) of the BuTaKli project in Freiamt within the Black Forest (Southwestern Germany) region (Magh et al., 2018). In general, the uppermost layer is drying out fastest especially during summertime, while lower layers, i.e. below 30 cm, retain a higher SWC_v for a longer time period. This implies different effects on the tree species with different rooting depths and thus access to soil water. Regarding the effect of SM on isoprenoid emissions - i.e. the γ factor - the γ_{SM} values for one vegetation period (during 2016) are shown in Fig. 7. Individual plots represent the SWC_v emission effects of different compounds or compound classes and different colours illustrate the SWC_v based values for three different depths. Apparently during summertime, when the evapotranspiration flux and the emission rates are highest due to elevated temperatures and radiation intensity, the effect is most intense. During the rather well watered summer 2016 γ_{SM}(isop) caused reduction by almost 40% for more shallow rooting species and by 20 to 30% for trees with access to deeper soil layers (60 cm in depth). γ_{SM}(MT) declined to nearly 55% on average with short time access to more water for deeper roots and γ_{SM}(SQT) to nearly 60% of emission rates.

During 2017 with an improved roof cover, the differences between different soil depths became more obvious, and they exceed effect changed by 10% or more between 40 and 60 cm in depth (not shown, (Magh et al., in prep.). Those effects are estimated to intensify remarkably during extensive drought periods such as occurred in summer 2018, of which no dataset is available. This is going to take down most of the BVOC emission rates with progressing drought period time, depending on the tree species rooting depth and soil water access. Therefore, the total sum of isoprenoid emissions of a specific forest ecosystem will be reflected by the individual contribution of tree species and its specific emission pattern, and the sum of *SM* affects the drought sensitivity of the ecosystem.

4 Conclusions

In this study we derived three sets of parameterizations for the influence of soil moisture on isoprenoid emission rates. Those depend on the details of soil characteristics, plant properties of on- and offline production of isoprenoids and potential defensive plant feedback mechanisms on oxidative stress. The effect on isoprene emissions acts similar as a small molecule able to penetrate the plant surface acting like a biological growth stress. While the *cuticula* provides some minor resistance it cannot

hinder isoprene from penetration at nearly closed stomata. Thus, the present description allows minor isoprene emissions below the *PWP*. The influence of soil water access on larger isoprenoid emission occurs on a notably larger range of $SWA_\%$ as a function of stomata opening (hydraulic conductivity pattern). Depending on the specific tree species some molecular structures of terpenes e.g. the more reactive ones like α-pinene and β-myrcene (Haberstroh et al., 2018; Ormeño et al., 2007)

5 and α-farnesene (Duhl et al., 2008; Haberstroh et al., 2018) display an elevated relative terpene flux contribution at lower soil moisture (Figs. S3-S8), indicating a defensive strategy of plants against oxidative stress at lower soil water concentrations, thus warmer conditions and in total critical for the plants survival. This is plant species dependent and can be incorporated by a secondary maximum close to the permanent wilting point. The named $SWA_\%$ impact on isoprenoid emission rates is expected to induce several feedback processes in the atmosphere and climate system including local tropospheric ozone

10 production and sink (Seinfeld and Pandis, 2016), new particle formation (Bonn et al., 2014; Bonn, 2014) and growth as well as cloud condensation nuclei (Bonn, 2014; Seinfeld and Pandis, 2016).With these findings we conclude that more studies on available soil water dependence of emissions of higher terpenes, oxygenates and follow-up processes, are essentially needed for different environments to realistically describe the natural feedback processes of forests and ecosystems in changing climate conditions and the anthropogenic impact on these. Because of that, the $SWA_\%$ concepts described should definitely be included

15 in corresponding global atmospheric chemistry transport models in order to cover not only plant response to the expected increase in drought periods but to future development of biosphere-atmosphere processes, resulting in adaptation or extinction in a changing climate.

Author contributions. B.B. was responsible for the methodology, analysis and writing. R.-K.M. conducted the SWC_v measurements and soil texture analysis, contributed to the data analysis and parameterization approach and was responsible for the soil water concepts. The formal

20 analysis of *Fagus sylvatica* BVOC emissions and water potential measurements at the campus field site was done by J.R. J.K. contributed by conceptualization of the *Fagus sylvatica* campus field site experiment, discussion about accurate plant physiology process description as well as review and editing.

Competing interests. There are no competing interests.

Acknowledgements. Funding within the German Waldklimafond project BuTaKli (no. 100261371) is kindly acknowledged. Highly acknowl-

25 edged is the supply of SWC_v data for Campus Flugplatz soil texture by Angelika Küberts and Simon Haberstrohs support with further information and data on the Haberstroh et al. (2018) measurements. Thanks go to the supporting staff and colleagues at Freiburg University and to all partners within the BuTaKli project for their nice support and exchange of information and data, too. We thank the R Development Core Team for providing version 3.5.1 with its individual tool packages (R Core Team, 2017), which were used for conducting this study.

References

Atkinson, R., Hasegawa, D., and Aschmann, S. M. Rate constants for the gas-phase reactions of O3 with a series of monoterpenes and related compounds at 296±2 K. *Int. J. Chem. Kinet.*, **22**, 871-887, 1990.

Atkinson, R., and Arey, J. Gas-phase tropospheric chemistry of biogenic volatile organic compounds: a review. *Atmos. Environ.*, **37**, S197-S219, 2003, doi: 10.1016/S1352-2310(03)00391-1.

Blume, H.-P.; Brümmer, G. W.; Horn, R., Kandeler, E., Kögel-Knabner, I., Kretzschmar, R., Stahr, K., Wilke, B.-M., Thiele-Bruhn, S., and Welp, G. *Scheffer/Schachtschabel: Lehrbuch der Bodenkunde*, Spektrum Akad. Verlag. p.570, Heidelberg, 2010.

Bonn, B., Bourtsoukidis, E., Sun, T. S., Bingemer, H., Rondo, L., Javed, U., Li, J., Axinte, R,; Li, X., Brauers, T., Sonderfeld, H., Koppmann, R., Sogachev, A., Jacobi, S., and Spracklen, D. V. The link between atmospheric radicals and newly formed particles at a spruce forest site in Germany. *Atmos. Chem. Phys.*, **14**, 10823–10843, 2014, doi: 10.5194/acp-14-10823-2014.

Bonn, B. *Biogene Terpenemissionen und sekundäre Aerosolpartikelbildung: Ein Weg von Nadelwäldern Klimaückkopplungsprozesse zu steuern.* Prof. thesis, J. W. Goethe Universität, p.336, Frankfurt/Main, 2014.

Bonn, B., Kreuzwieser, J., Sander, F., Yousefpour, R., Baggio, T., and Adewale, O. The uncertain role of biogenic VOC for boundary-layer ozone concentration: Example investigation of emissions from two forest types with a box model. *Climate*, **5**, 78-98, 2017, doi:10.3390/cli5040078.

Bonn, B., Sperlich, D., Schindler, D., Magh, R.-K., Grote, R., Rehschuh, S., Dannenmann, M., Kreuzwieser, J., Rennenberg, H., Trautmann, R., and Yousefpour, R. Counteracting climate change: The impacts of intermixing European beech forests with silver fir on the radiation regime in Southwestern Germany. *Atmos. Environ.*, in prep.

Bourtsoukidis, E., Bonn, B., Dittmann, A., Hakola, H., Hellén, H., and Jacobi, S. Ozone stress as a driving force of sesquiterpene emissions: A suggested parameterisation. *Biogeosciences*, **9**, 4337–4352, 2012, doi: 10.5194/bg-9-4337-2012.

Bourtsoukidis, E., Kawaletz, H., Radacki, D., Schütz, S., Hakola, H., Hellén, H., Noe, S., Mölder, I., Ammer, C., and Bonn, B. Impact of flooding and drought conditions on the emission of volatile organic compounds of *Quercus robur* and *Prunus serotina. Trees - Struct. Funct.*, **28**, 193–204, 2014, doi: 10.1007/s00468-013-0942-5.

Brilli, F., Barta, C., Fortunati, A., Lerdau, M., Loreto, F., and Centritto, M. Response of isoprene emission and carbon metabolism to drought in white poplar (*Populus alba*) saplings. *New Phytol.*, **175**, 244–254, 2007, doi: 10.1111/j.1469-8137.2007.02094.x.

Chen, F., and Dudhia, J. Coupling an advanced land surface-hyrology model with the Penn State NCAR MM5 modeling system. Part 1: Model implementation and sensitivity. *Mon. Weather Rev.*, **129**, 569–585, 2001, doi: 10.1175/1520-0493(2001)129<0569:CAALSH>2.0.CO;2.

Dalsgaard, L., Mikkelsen, T. N., and Bastrup-Birk, A. Sap flow for beech (*Fagus sylvatica L.*) in a natural and a managed forest - Effect of spatial heterogeneity. *J. Plant Ecol.*, **4**, 23–35, 2011, doi: 10.1093/jpe/rtq037.

Duhl, T. R., Helmig, D., and Guenther, A. Sesquiterpene emissions from vegetation: A review. *Biogeosciences*, **5**, 761–777, 2008, doi: 10.5194/bg-5-761-2008.

Fall, R., and Monson, R. K. Isoprene emission rate and intercellular isoprene concentration as influenced by stomatal distribution and conductance. *Plant Physiol.*, **100**, 987-992, 1992, doi: 10.1104/pp.100.2.987.

Fortunati, A., Barta, C., Brilli, F., Centritto, M., Zimmer, I., Schnitzler, J. P., and Loreto, F. Isoprene emission is not temperature-dependent during and after severe drought-stress: A physiological and biochemical analysis. *Plant J.*, **55**, 687–697, 2008, doi: 0.1111/j.1365-313X.2008.03538.x.

Genard-Zielinski, A. C., Boissard, C., Ormeño, E., Lathière, J., Reiter, I. M., Wortham, H., Orts, J. P., Temime-Roussel, B., Guenet, B., Bartsch, S., Gauquelin, T., and Fernandez, C. Seasonal variations of *Quercus pubescens* isoprene emissions from an in natura forest under drought stress and sensitivity to future climate change in the Mediterranean area. *Biogeosciences*, **15**, 4711–4730, 2018, doi: 10.5194/bg-15-4711-2018.

5   Gessler, A., Keitel, C., Kreuzwieser, J., Matyssek, R., Seiler, W., and Rennenberg, H. Potential risks for European beech (*Fagus sylvatica L.*) in a changing climate. *Trees - Struct. Funct.*, **21**, 1–11, 2007, doi: 10.1007/s00468-006-0107-x.

Ghirardo, A., Koch, K., Taipale, R., Zimmer, I., Schnitzler, J. P., and Rinne, J. Determination of *de novo* and pool emissions of terpenes from four common boreal/alpine trees by $^{13}CO_2$ labelling and PTR-MS analysis. *Plant, Cell Environ.*, **33**, 781–792, 2010, doi: 10.1111/j.1365-3040.2009.02104.x.

10   Goldstein, A. H., and Galbally, I. E. Known and unexplored organic constituents in the Earth's atmosphere. *Environ. Sci. Technol.*, **41**, 1514–1521, 2007, doi: 10.1021/es072476p.

Guenther, A., Hewitt, C. N., Erickson, D., Fall, R., Geron, C., Graedel, T., Harley, P., Klinger, L., Lerdau, M., McKay, W. A., Pierces, T., Scholes, B., Steinbrecher, R., Tallamraju, R., Taylor, J., and Zimmerman, P. A global model of natural volatile organic compound emissions. *J. Geophys. Res.*, **100**, 8873–8892, 1995, doi: 10.1029/94JD02950.

15   Guenther, A., Karl, T., Harley, P., Wiedinmyer, C., Palmer, P. I., and Geron, C. Estimates of global terrestrial isoprene emissions using MEGAN (Model of Emissions of Gases and Aerosols from Nature). *Atmos. Chem. Phys.*, **6**, 3181-3210, 2006, doi; 10.5194/acp-6-3181-2006.

Guenther, A. B., Jiang, X., Heald, C. L., Sakulyanontvittaya, T., Duhl, T., Emmons, L. K., and Wang, X. The Model of Emissions of Gases and Aerosols from Nature Version 2.1 (MEGAN2.1): An extended and updated framework for modeling biogenic emissions. *Geosci.*

20   *Model Dev.*, **5**, 1471–1492, 2012, doi; 10.5194/gmd-5-1471-2012.

Haberstroh, S., Kreuzwieser, J., Lobo-do-Vale, R., Caldeira, M. C., Dubbert, M., and Werner, C. Terpenoid emissions of two Mediterranean woody species in response to drought stress. *Front. Plant Sci.*, **9**, 1–17, 1071, 2018, doi: 10.3389/fpls.2018.01071.

Hansen, U., and Seufert, G. Terpenoid emission from *Citrus sinensis* (L.) OSBECK under drought stress. *Phys. Chem. Earth, Part B Hydrol. Ocean. Atmos.*, **42**, 681-687, 1999, doi: 10.1016/S1464-1909(99)00065-9.

25   Höferl, M., Stoilova, I., Wanner, J., Schmidt, E., Jirovetz, L., Trifonova, D., Stanchev, V., and Krastanov, A. Composition and Comprehensive Antioxidant Activity of Ginger (*Zingiber officinale*) Essential oil from Ecuador. *Nat. Prod. Commun.*, **10**, 1085-1090, 2015, ISSN: 1934-578X, 1555-9475.

Holopainen, J. K., Kivimäenpää, M., and Nizkorodov, S. A. Plant-derived secondary organic material in the air and ecosystems. *Trends Plant Sci.*, **22**, 744-753, 2017, doi: 10.1016/j.tplants.2017.07.004.

30   IPCC, 2014. Climate Change 2014: *Synthesis Report. Contribution of Working Groups I, II and III to the Fifth Assessment Report of the Intergovernmental Panel on Climate Change*, Core Writing Team, R.K. Pachauri and L.A. Meyer (eds.). IPCC, Geneva, Switzerland, 151 pp.

Kändler, G., and Cullmann, D. *Regionale Auswertung der Bundeswaldinventur Wuchsgebiet Schwarzwald.* 2016.

Kaurinovic B., Vlaisavljevic, S., Popovic, M., Vastag, D., and Djurendic-Brenesel, M. Antioxidant properties of *Marrubium peregrinum* L.

35   (*Lamiaceae*) essential oil. *Molecules*, **15**, 5943-5955, 2010, ISSN: 1420-3049.

Keuler, K., Radtke, K., Kotlarski, S., and Lüthi, D. Regional climate change over Europe in COSMO-CLM: Influence of emission scenario and driving global model. *Meteorol. Z.*, **25**, 121–136, 2016, doi: 10.1127/metz/2016/0662.

Kleiber, A., Duan, Q., Jansen, K., Junker, L. V., Kammerer, B., Rennenberg, H., Ensminger, I.;,Gessler, A., and Kreuzwieser, J. Drought effects on root and needle terpenoid content of a coastal and an interior douglas fir provenance. *Tree Physiol.*, **37**, 1648-1658, 2017, doi: 10.1093/treephys/tpx113.

Kosina, J., Dewulf, J., Viden, I., Pokorska, O., and Van Langenhove, H. Dynamic capillary diffusion system for monoterpene and sesquiterpene calibration: Quantitative measurement and determination of physical properties. *Int. J. Environ. An. Ch.*, **93**, 1-13, 2012, doi: 10.1080/03067319.2012.656621.

Kreienkamp, F., Paxian, A., Früh, B., Lorenz, P., and Matulla, C. Evaluation of the empirical–statistical downscaling method EPISODES. *Clim. Dynam.*, ISSN: 1432-0894, 2018, pp.36, doi: 10.1007/s00382-018-4276-2.

Lappalainen, H. K., Sevanto, S., Bäck, J., Ruuskanen, T. M., Kolari, P., Taipale, R., Rinne, J., Kulmala, M., and Hari, P. Day-time concentrations of biogenic volatile organic compounds in a boreal forest canopy and their relation to environmental and biological factors. *Atmos. Chem. Phys.*, **9**, 5447–5459, 2009, doi: 10.5194/acp-9-5447-2009.

Laothawornkitkul, J., Taylor, J. E., Paul, N. D., and Hewitt, C. N. Biogenic volatile organic compounds in the Earth system: Tansley review. *New Phytol.*, **183**, 27–51, 2009, doi: 10.1111/j.1469-8137.2009.02859.x.

Lavoir, A. V., Staudt, M., Schnitzler, J. P., Landais, D., Massol, F., Rocheteau, A., Rodriguez, R., Zimmer, I., and Rambal, S. Drought reduced monoterpene emissions from the evergreen Mediterranean oak *Quercus ilex*: Results from a throughfall displacement experiment. *Biogeosciences*, **6**, 1167–1180, 2009, doi: 10.5194/bg-6-1167-2009.

Leij, F. J., Alves, W. J., van Genuchten, M. T., and Williams, J. R. *Unsaturated Soil Hydraulic Database, UNSODA 1.0 User's Manual*, 1996.

Loreto, F., and Velikova, V. Isoprene produced by leaves protects the photosynthetic apparatus against ozone damage, quenches ozone products, and reduces lipid peroxidation of cellular membranes. *Plant Physiol.*, **127**, 1781-1787, 2001, doi:10.1104/pp.010497.

Lüpke, M., Leuchner, A., Steinbrecher, R., and Menzel, A. Impact of summer drought on isoprenoid emissions and carbon sink of three Scots pine provenances. *Tree Physiol.*, **36**, 1382–1399, 2016, doi:10.1093/treephys/tpw066

Lüpke, M., Leuchner, M., Steinbrecher, R., and Menzel, A. Quantification of monoterpene emission sources of a conifer species in response to experimental drought. *AoB Plants*, **X**, plx045, 2017a, doi: 10.1093/aobpla/plx045.

Lüpke, M., Steinbrecher, R., Leuchner, M., and Menzel, A. The Tree Drought Emission MONitor (Tree DEMON), an innovative system for assessing biogenic volatile organic compounds emission from plants. *Plant Methods*, **13**, 14, 2017b, doi: 10.1186/s13007-017-0166-6.

Magh, R.-K., Yang, F., Rehschuh, S., Burger, M., Dannenmann, M., Pena, R., Burzlaff, T., Ivanković, M., and Rennenberg, H. Nitrogen nutrition of European beech is maintained at sufficient water supply in mixed beech-fir stands. *Forests*, **9**, 733, 2018, doi:10.3390/f9120733.

Magh, R.-K., Eiferle, C., Dannenmann, M., Rennenberg, H.Dubbert, M., and Dubbert, M.Rennenberg, H. Water use strategies of beech and silver fir in a temperate forest after prolonged droughtuptake relationships in pure and mixed beech – fir stands as affected by summer drought. *J. Hydrol., in prep.*

Manninen, A. M., Vuorinen, M., and Holopainen, J. K. Variation in growth, chemical defense, and herbivore resistance in Scots pine provenances. *J. Chem. Ecol.*, **24**, 1315-1331, 1998, doi: 10.1023/A:1021222731991.

McGillen, M. R., Ghalaieny, M., and Percival, C. J. Determination of gas-phase ozonolysis rate coefficients of C8-14 terminal alkenes at elevated temperatures using the relative rate method. *Phys. Chem. Chem. Phys.*, **13**, 10965–10969, 2011, doi: 10.1039/c0cp02643c.

Mogensen, D., Gierens, R., Crowley, J. N., Keronen, P., Smolander, S., Sogachev, A., Nölscher, A. C., Zhou, L., Kulmala, M., Tang, M. J., Williams, J., and Boy, M. Simulations of Atmospheric OH, O_3 and NO_3 reactivities within and above the Boreal Forest. *Atmos. Chem. Phys.*, **15**, 3909-3932, 2015, doi: 10.5194/acp-15-3909-2015.

Moukhtar, S., Bessagnet, B., Rouil, L., and Simon, V. Monoterpene emissions from beech (*Fagus sylvatica*) in a French forest and impact on secondary pollutants formation at regional scale. *Atmos. Environ.*, **39**, 3535–3547, 2005, doi: 10.1016/j.atmosenv.2005.02.031.

Moukhtar, S., Couret, C., Rouil, L., and Simon, V. Biogenic volatile organic compounds (BVOCs) emissions from *Abies alba* in a French forest. *Sci. Total Environ.*, **354**, 232–245, 2006, doi: doi:10.1016/j.scitotenv.2005.01.044.

Münz, J. *Entwicklung einer Thermodesorptionseinheit für die GC/MS zur Bestimmung hochreaktiver, biogener Kohlenwasserstoffe und deren Anwendung im Rahmen von Labor- und Feldstudien.* PhD thesis, J. Gutenberg Universität, Mainz, 196 p., 2010.

Neeb, P. Structure-reactivity based estimation of the rate constants for hydroxyl radical reactions with hydrocarbons. *J. Atmos. Chem.*, **35**, 295–315, 2000, doi: 10.1023/A:1006278410328.

Niinemets, Ü. Mild versus severe stress and BVOCs: Thresholds, priming and consequences. *Trends Plant Sci.*, **15**, 145-153, 2010, doi: 10.1016/j.tplants.2009.11.008.

Niinemets, Ü. Responses of forest trees to single and multiple evironmental stresses from seedlings to mature plants: Past stress history, stress interactions, tolerance and acclimation. *Forest Ecol. Manage.*, **260**, 1623-1639, 2010, doi: 10.1016/j.foreco.2010.07.054.

Niinemets, Ü., Fares, S., Harley, P., and Jardine, K. J. Bidirectional exchange of biogenic volatiles with vegegation: Emission sources, reactions, breakdown and deposition. *Plant Cell Environ.*, **37**, 1790-1809, 2014, doi: 10.1111/pce.12322.

Nölscher, A. C., Butler, T., Auld, J., Veres, P., Muñoz, A., Taraborrelli, D., Vereecken, L., Lelieveld, J., and Williams, J. Using total OH reactivity to assess isoprene photooxidation via measurement and model. *Atmos. Environ.*, **89**, 453-463, 2014, doi: 10.1016/j.atmosenv.2014.02.024.

Nölscher, A. C., Yañez-Serrano, A. M., Wolff, S., De Araujo, A. C., Lavric, J. V., Kesselmeier, J., and Williams, J. Unexpected seasonality in quantity and composition of Amazon rainforest air reactivity. *Nat. Commun.*, **7**, 10383, 2016, doi: 10.1038/ncomms10383.

Oikawa, P. Y., and Lerdau, M. T. Catabolism of volatile organic compounds influences plant survival. *Trends Plant Sci.*, **18**, 695–703, 2013, doi: 10.1016/j.tplants.2013.08.011.

Ormeño, E., Mévy, J. P., Vila, B., Bousquet-Mélou, A., Greff, S., Bonin, G., and Fernandez, C. Water deficit stress induces different monoterpene and sesquiterpene emission changes in Mediterranean species. Relationship between terpene emissions and plant water potential. *Chemosphere*, **67**, 276–284, 2007, doi: 10.1016/j.chemosphere.2006.10.029.

Parveen, S., Harun-Ur-Rashid, Md., Inafuku, M., Iwasaki, H., and Oku, H. Molecular regulatory mechanism of isoprene emission under shortterm drought stress in the tropical tree *Ficus septica*. *Tree Phys.*, **39**, 440-453, doi: 10.1093/treephys/tpy123.

Pegoraro, E., Rey, A., Bobich, E. G., Barron-Gafford, G., Grieve, K. A.; Malhi, Y., and Murthy, R. Effect of elevated CO_2 concentration and vapour pressure deficit on isoprene emission from leaves of populus deltoides during drought. *Funct. Plant Biol.*, **31**, 1137–1147, 2004, doi: 10.1071/FP04142.

Pegoraro, E., Rey, A., Greenberg, J., Harley, P., Grace, J., Malhi, Y., and Guenther, A. Effect of drought on isoprene emission rates from leaves of *Quercus virginiana Mill. Atmos. Environ.*, **38**, 6149–6156, 2004, doi: 10.1016/j.atmosenv.2004.07.028.

Peñuelas, J., and Staudt, M. BVOCs and global change. *Trends Plant Sci.*, **15**, 133-144, 2010, doi: 10.1016/j.tplants.2009.12.005.

Piechowiak, T., Antos, P., Kosowski, P., Skrobacz, K., Józefczyk, R., and Balawejder, M. Impact of ozonation process on the microbiological and antioxidant status of raspberries (*Rubus ideaeus* L.) during storage at room temperature. *Agr. Food Sci.*, **28**, 35-44, doi:10.23986/afsci.70291.

R Core Team. *R: A Language and Environment for Statistical Computing.* R foundation for statistical Computing: Vienna, Austria, 2017.

Rennenberg, H., Loreto, F., Polle, A., Brilli, F., Fares, S., Beniwal, R. S., and Gessler, A. Physiological responses of forest trees to heat and drought. *Plant Biol.*, **8**, 556-571, 2006, doi: 10.1055/s-2006-924084.

[RC1 7
L.158ff

[RC1 8
L.158ff

Rombach, J. *Einfluss reduzierter Wasserverfügbarkeit auf die VOC-Emissionen bei Buchen*, Albert-Ludwigs Universität, Freiburg, 2018, 13, 14 ~~doi: 10.1186/s13007-017-0166-6, 2018~~.

Sander, R. Compilation of Henry's law constants (version 4.0) for water as solvent. *Atmos. Chem. Phys.*, **15**, 4399–4981, 2015, doi:10.5194/acp-15-4399-2015.

5   Saunier, A., Ormeño, E., Wortham, H., Temime-Roussel, B., Lecareux, C., Boissard, C., and Fernandez, C. Chronic drought decreases anabolic and catabolic BVOC emissions of *Quercus pubescens* in a Mediterranean forest. *Front. Plant Sci.*, **8**, 71, 2017, doi: 10.3389/fpls.2017.00071.

Schölzel, C., and Hense, A. Probabilistic assessment of regional climate change in Southwest Germany by ensemble dressing. *Clim. Dyn.*, **36**, 2003–2014, 2011, doi 10.1007/s00382-010-0815-1.

10   Scholander, P. F. The role of solvent pressure in osmotic systems. *P. Natl. Acad. Sci.*, **55**, 1407–1414, 1966.

Seinfeld, J. H., and Pandis, S. N. *Atmospheric Chemistry and physics: From air pollution to climate change.* 3rd ed., Wiley Intersci., Hoboken, 2016, p.1152, ISBN: 978-1-118-94740-1.

Šimpraga, M., Verbeeck, H., Demarcke, M., Joó, É.; Pokorska, O., Amelynck, C., Schoon, N., Dewulf, J., van Langenhove, H., Heinesch, B., Aubinet, M., Laffineur, Q., Müller, J.-F., and Steppe, K. Clear link between drought stress, photosynthesis and biogenic volatile organic

15   compounds in *Fagus sylvatica L. Atmos. Environ.*, **45**, 5254-5259, 2011, doi: 10.1016/j.atmosenv.2011.06.075.

Simpson, J. R., Fritschen, L. J., and Walker, R. B. Estimating stomatal diffusion resistance for douglas-fir, lodgepole pine and white oak under light saturated conditions. *Agric. For. Meteorol.*, **33**, 299–313, 1985, doi: 10.1016/0168-1923(85)90030-9.

US EPA, *Estimation Programs Interface Suite™ for Microsoft Windows, v. 4.11*. United States Environmental Protection Agency, Washington, DC, USA, 2018. (https://www.epa.gov/tsca-screening-tools/download-epi-suitetm-estimation-program-interface-v411)

20   van Genuchten, M. T. A closed-form equation for predicting the hydraulic conductivity of unsaturated soils. *Soil Sci. Soc. Am. J.*, **44**, 892–898, 1980.

Yalcinkaya, T., Uzilday, B., Ozgur, R., Turkan, I., and Mano, J. Lipid peroxidation-derived reactive carbonyl species (RCS): Their interaction with ROS and cellular redox during environmental stresses. *Environ. Exp. Bot.*, **165**, 139-149, doi: 10.1016/j.envexpbot.2019.06.004.

[RC2 16
L.344

[RC1 9
L.158ff
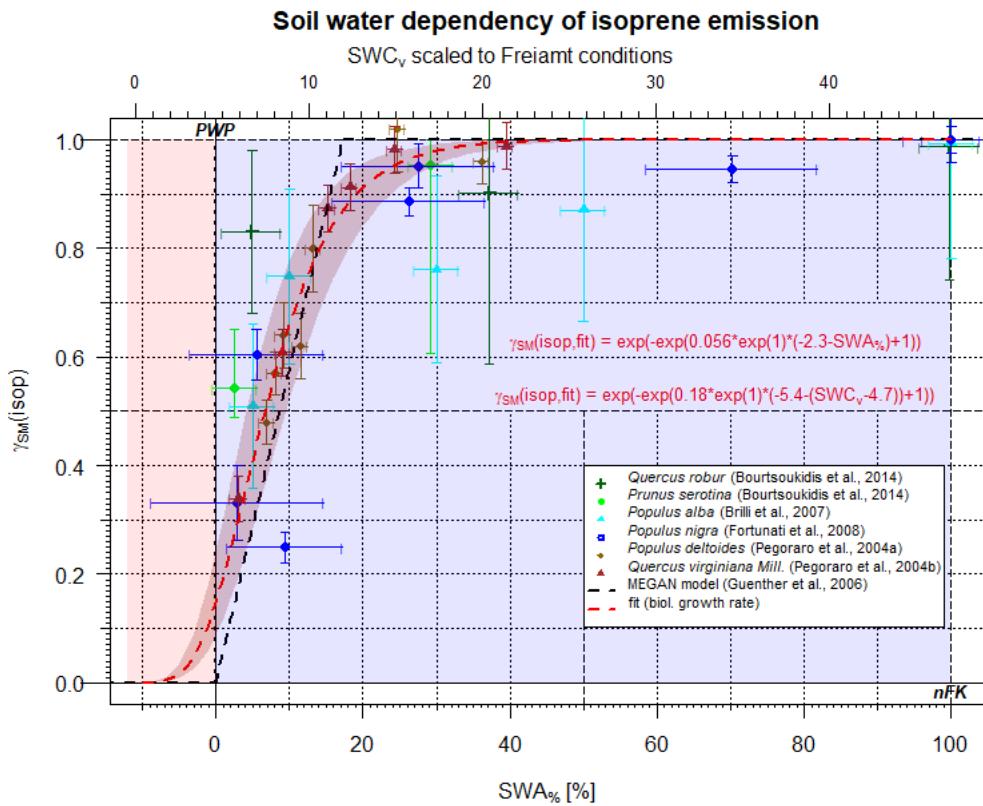
Figure 1. Scaling parameter γ_{SM}(isop) for the effect of soil moisture on isoprene emissions as a function of $SWA_\%$ (lower x-axis) and for comparison the SWC_v for a selected condition (upper horizontal axis). Data points represent observations, and different colours refer to different studies. The black dashed line displays the approach by Guenther et al. (2006, 2012), the red one the present form.
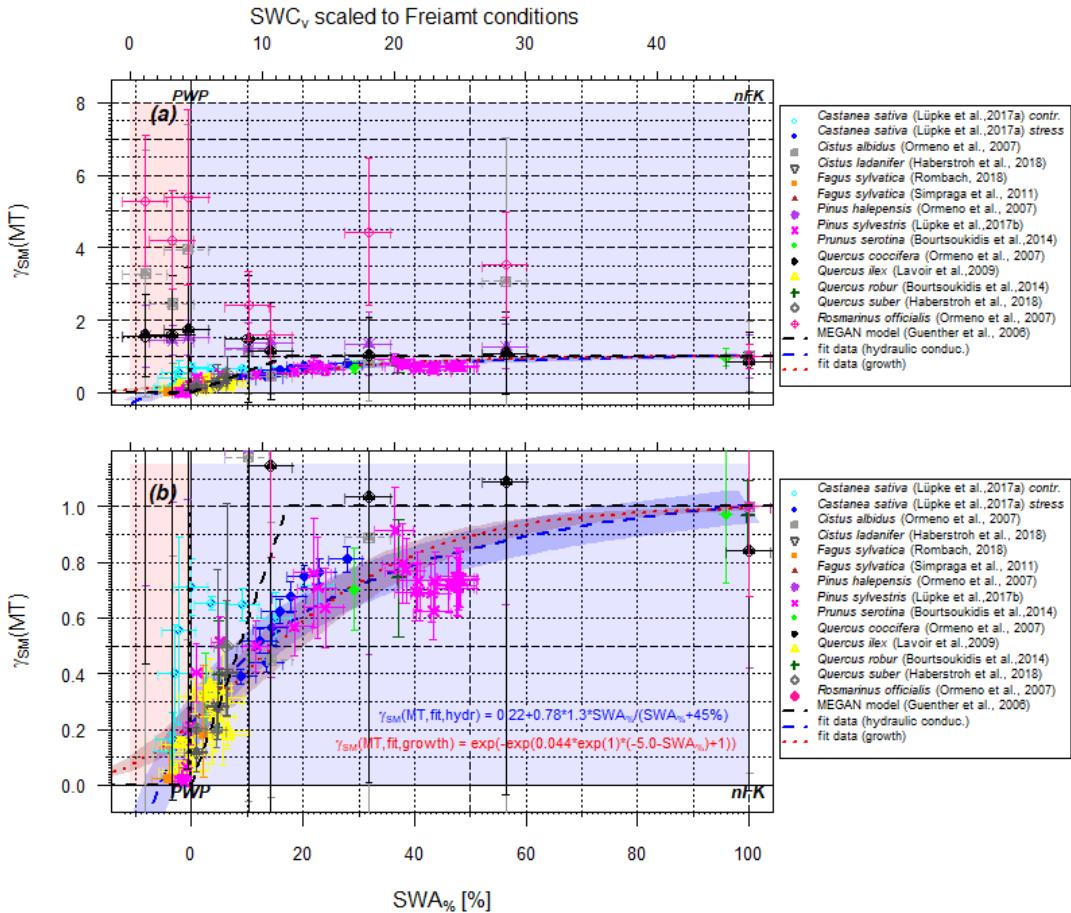
Figure 2. Scaling parameter γ_{SM}(MT) for the effect of soil moisture on isoprene emissions as a function of $SWA_\%$ (lower x-axis) and for comparison the SWC_v for a selected condition (upper horizontal axis). The upper plot (a) displays the full data range, while the lower plot (b) zooms vertical area between 0 and 1.2. Data points represent observations, and different colours refer to different studies. The black dashed line displays the approach by Guenther et al. (2006, 2012) for isoprene only[RC2], the red one the present form using hydraulic conductivity as driving force and the darkred one the biological growth stress as driving force.
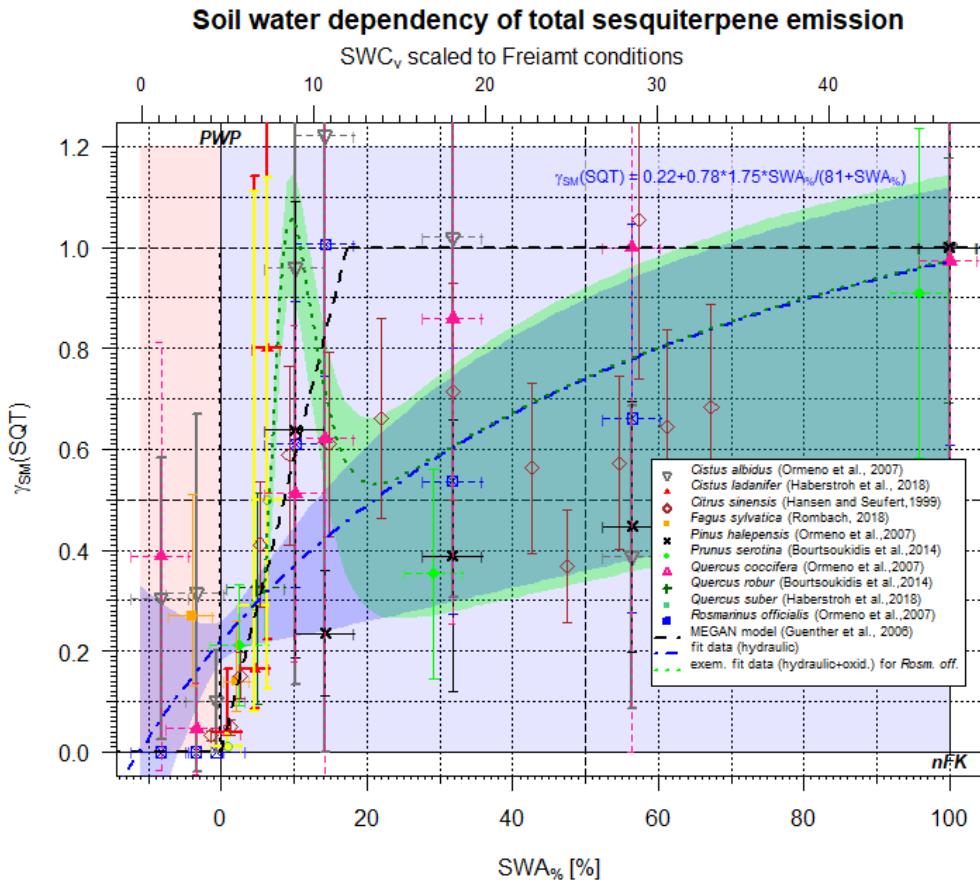
Figure 3. Scaling parameter $\gamma_{SM}(\text{SQT})$ for the effect of soil moisture on SQT emissions as a function of $SWA_\%$ (lower x-axis) and for comparison the SWC_v for a selected condition (upper horizontal axis). Data points represent observations, different colours refer to different studies. The black dashed line displays the approach by Guenther et al. (2006, 2012) for isoprene only[RC2], the blue one the present form. The green pointed line represents an exemplary fit to $\gamma_{SM}(\text{SQT})$ based on *Cistus* and *Rosmarinus officialis* data.
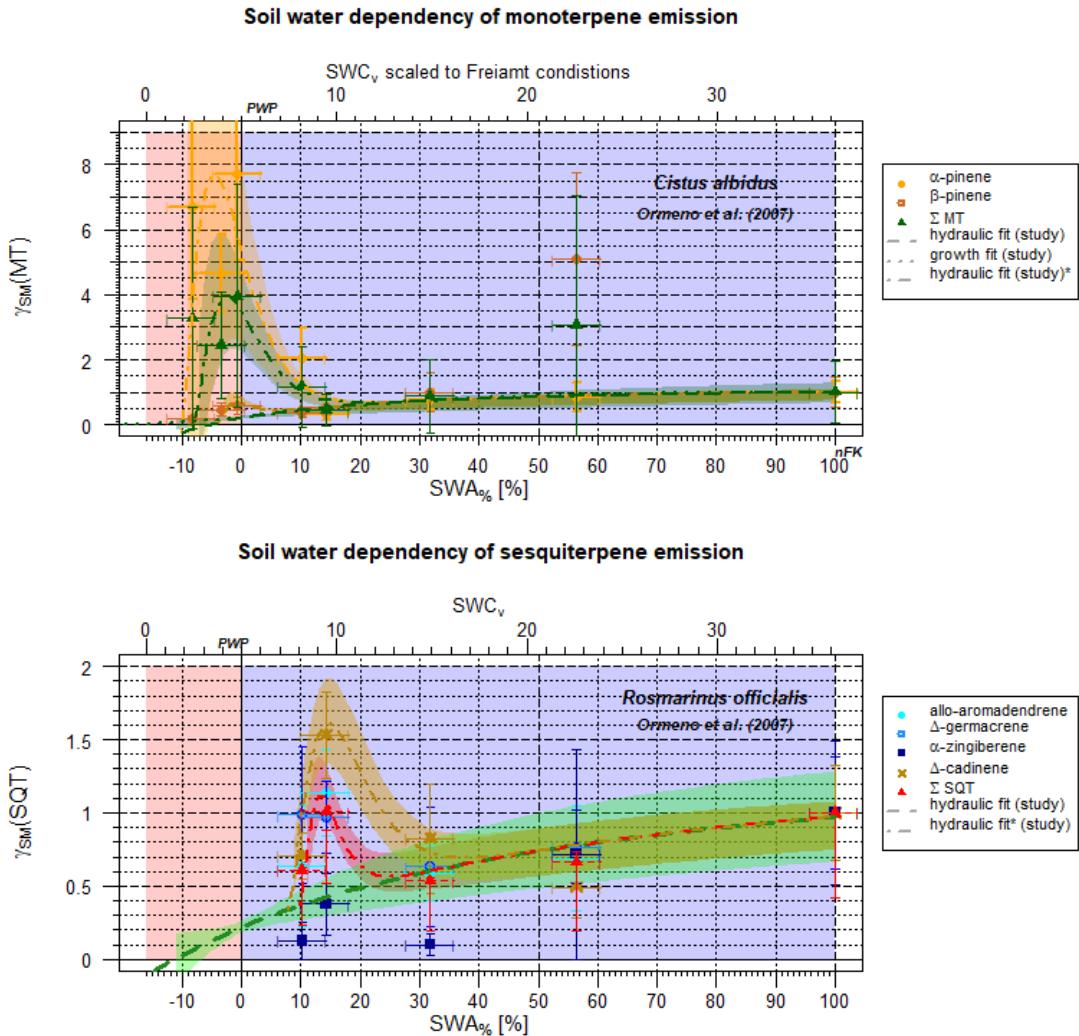
Figure 4. Exemplary scaling parameter γ_{SM} for the effect of soil moisture with a maximum at *PWP* on individual and total terpene emissions as a function of $SWA_\%$ (lower x-axis), and for comparing the SWC_v at Freiamt soil conditions (upper horizontal axis) (*Cistus albidus*) (Ormeño et al., 2007). Top plot: *SM* effect on monoterpene emission fluxes of individual structured monoterpenes, as well as of the total sum of monoterpenes; lower plot: the same for individual structures and total sum of sesquiterpene emissions (*Rosmarinus officialis*) (Ormeño et al., 2007).
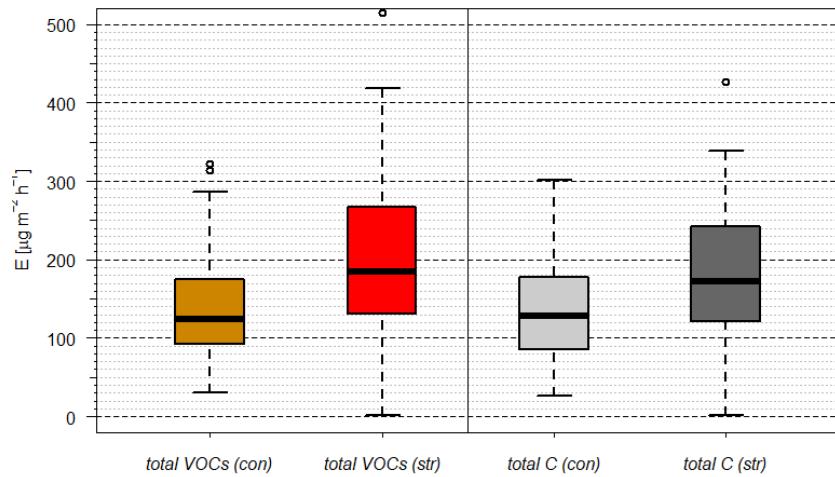
Figure 5. Change for the total sum of VOC (left) and total carbon (right)~~individual mono- and sesquiterpene species~~[RC2] emission fluxes of *Fagus sylvatica* for two *SM* conditions (Rombach, 2018). Because of not normal distributed data, values are stated as median and 25th (lower) and 75th (upper) percentiles.
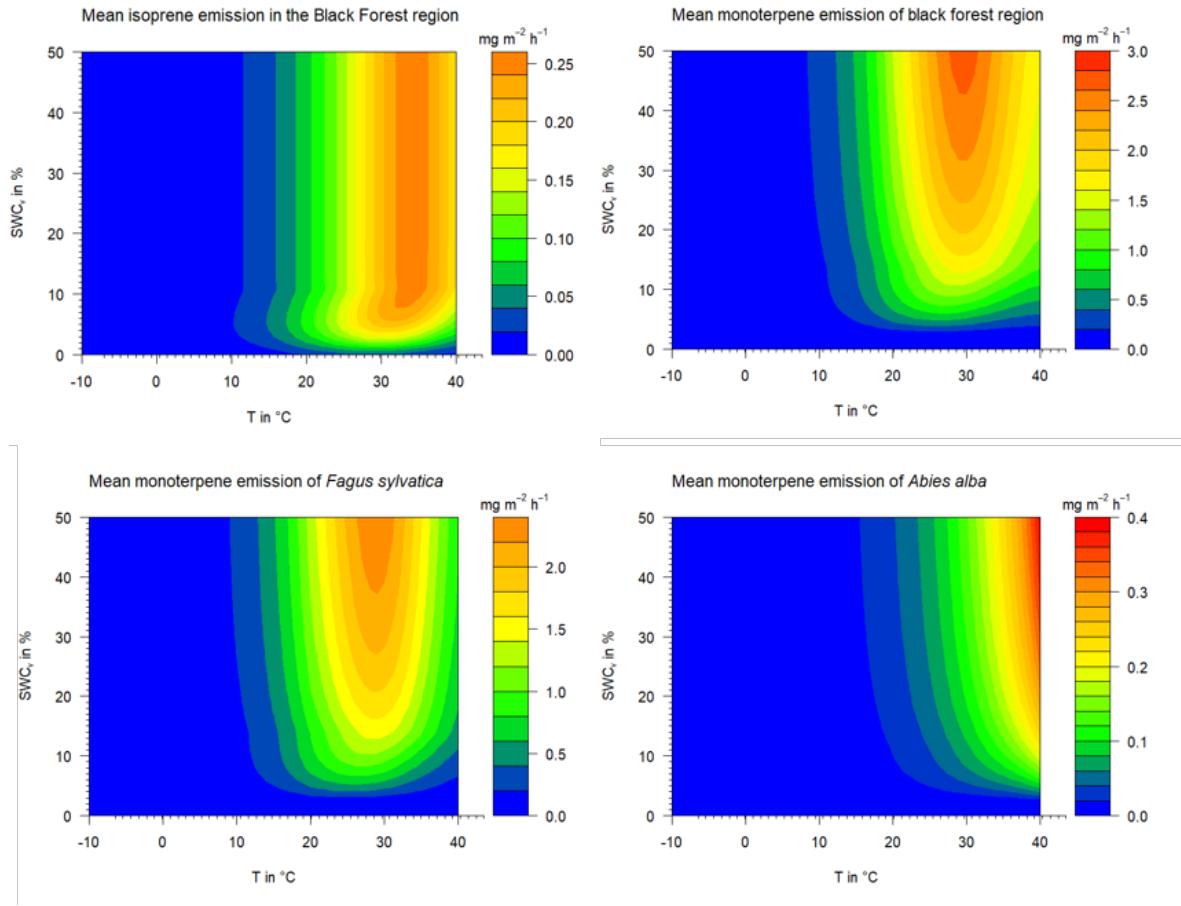
Figure 6. Calculated m~~M~~[RC2]ean isoprene and monoterpene emissions under different temperature and drought stress conditions using the parameterisations of Guenther et al. (2012) and the SWC dependency derived in this study[RC2]. "Black Forest region" represents the forest inventory mean tree species mixture of the Black Forest area. Upper left: total Isoprene emission, upper right: total monoterpene emission, baseline: *Fagus sylvatica* and *Abies alba* based MT emission rates (lower left and right).
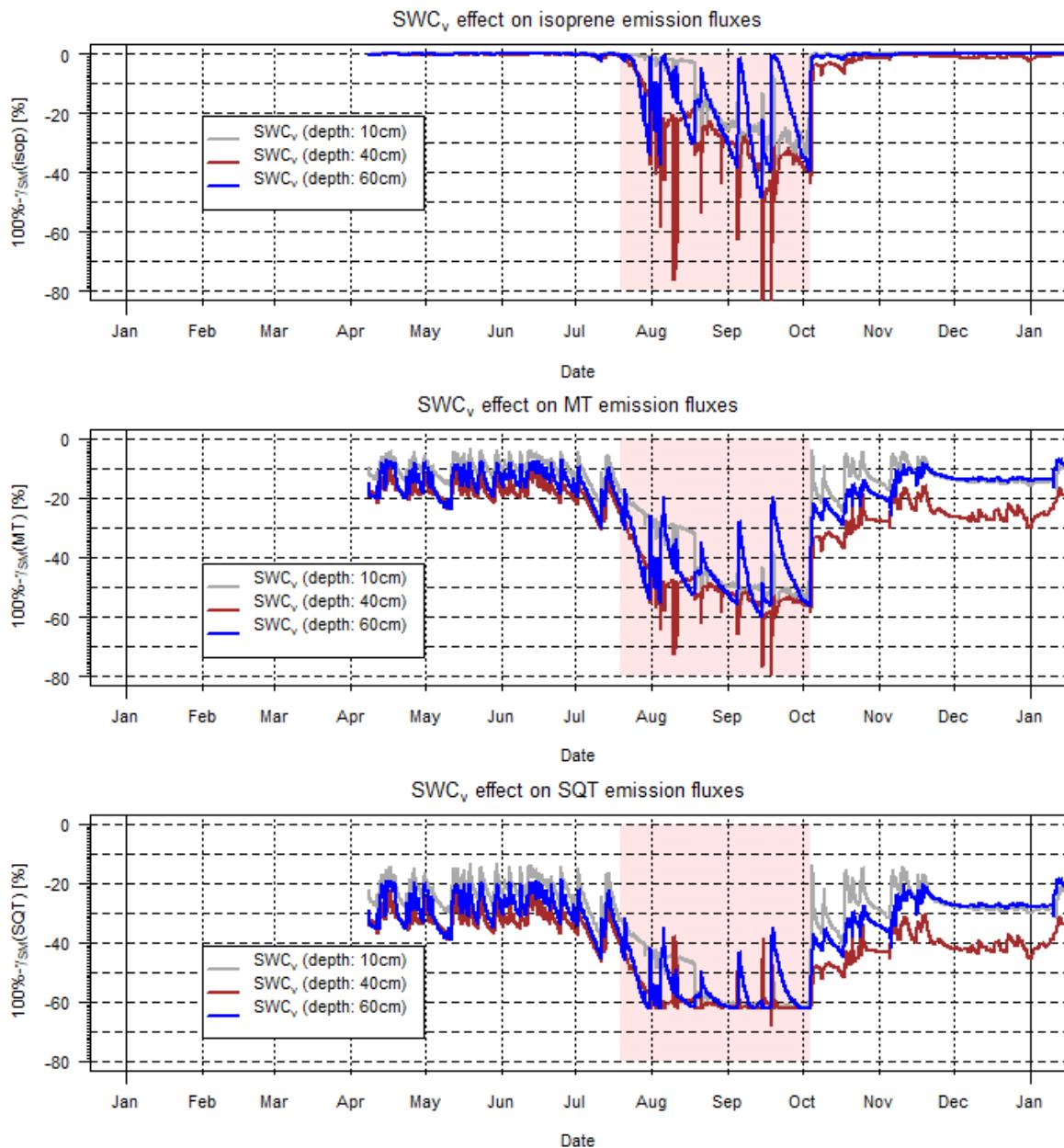
Figure 7. Calculated γ_{SM} effects during 2016 at Freiamt on isoprene, total MT and SQT emission rates. Note, two induced drought periods during summer and quite saturated conditions else when. The applied drought period is indicated by a reddish background.[RC2]

Table 1. Overview of abbreviated terms and parameter names

Abbreviation	Name	Abbreviation	Name
a,b,c	fitting parameters, indices 'g' and 'h' reflect growth and hydraulic conductivity based fits	NO_x	nitrogen oxides (=NO+NO$_2$)
β	temperature dependent increase of emission rates	*PAR*	photosynthetically active radiation
CCN	cloud condensation nuclei	*PWP*	permanent wilting point
E	emission rate of compound (class) [mg g(dw)$^{-1}$ h^{-1}]	*ROS*	reactive oxidation species
E_0	emission rate at standard cond.	*RSE*	residual standard error
$FASW_\%$	fraction of available soil water [%]	*SAR*	structure activity relationships
FK	field capacity	*SM*	soil moisture
γ_T, γ_L, γ_{CO2}, γ_{SM}	emission regulating factor for the impact of *T*, light, CO$_2$ and soil moisture	*SQT*	sesquiterpenes (C$_{15}$H$_{24}$)
$\gamma_{SM,g}$, $\gamma_{SM,h}$	γ_{SM} described by growth or hydraulic conductivity curve	$SWA_\%$, SWA_v	soil water availability, percentile [%] and volumetric [v]
k_{OH}, k_{O3}	reaction rate constants with OH and ozone	SWC_v, SWC_m	Soil water content volumetric [vol %] and by mass [mass %]
MT	monoterpenes (C$_{10}$H$_{15}$)	*VPD*	vapour pressure deficit
nFK	net field capacity	ψ, ψ_{pd}	matrix or water potential [MPa]

Table 2. Overview of studies, tree species and corresponding conditions as well as soil water parameters used for deriving the γ_{SM} parameterization for isoprene, MT and SQT emissions. References to the individual studies are listed in the final column. Soil water status parameters include the fraction of available soil water ($FASW$ in %), leaf water content, available soil water ($SWA_\%$ in %), soil water content by volume (SWC_v), by mass (SWC_m) and by the ratio water volume per soil mass (SWC_{vm}), stem diameter and water potential during daytime (ψ in MPa) and predawn (ψ_{PD} in MPa).

Tree species / Lat. name	engl. name	Soil type	PWP ass. [$m^3\ m^{-3}$]	VOC species classified	Parameter describing water status	Rewatering	environment	Reference
Castanea sativa (M)[RC2]	sw. chestnut	70% sand, 30% organic	2.8	different MTs	SWC_v	no	plant chamber	Lüpke et al. (2017a)
Cistus albidus (M)[RC2]	rockrose	calcareous soil	6.7	MTs, SQTs	p^{si}, SWC_{vm}	no	pots, greenhouse?	Ormeño et al. (2007)
Cistus ladanifer (M)[RC2]	common gum cistus	clay loam	10.2	Ox. MTs, MTs, SQTs, diterpenes	SWC_v, ψ	no	ambient	Haberstroh et al. (2018)
Cistus sinensis (M)[RC2]	orange	clay loam	10.9	trans-β-ocimene (MT), β-caryophyllene (SQTs)	SWC_v, ψ	yes	pot, greenhouse	Hansen and Seufert (1999)
Fagus sylvatica (T)[RC2]	European beech	CPS+fertilizer: 100% org?	6.0	total MTs	stem diameter	yes	growth room	Šimpraga et al. (2011)
Fagus sylvatica (T)[RC2]	European beech	Bedrock?	9.0±1.0	Isoprene, MTs, SQTs + 70 VOCs	Leaf water content, ψ_{PD} and ψ, SWC_v nearby	no	ambient	Rombach (2018)
Pinus sylvestris (T, A)[RC2]	pine	70% sand, 30% humus	2.8	1,8-cineole, different MTs	SWC_v	yes	plant chamber	Lüpke et al. (2017b)
Populus alba (T)[RC2]	white poplar	CPS: 100% org	6.0	Isoprene	$SWA_\%$	yes	growth chamber	Brilli et al. (2007)
Populus deltoids (T)[RC2]	cottonwood	60% bare soil, 40% organic	7.4	Isoprene	SWC_v, ψ_{PD}	no	greenhouse	Pegoraro et al. (2004a)
Populus nigra (T)[RC2]	black poplar	50% org, 50% sand	3.5	Isoprene	$FASW_\%$	yes	growth chamber	Fortunati et al. (2008)
Prunus serotina (T)[RC2]	cherry	70%, 30%	4.7	MTs, SQTs, OVOCs	$SWA_\%$	no	greenhouse	Boursoukidis et al. (2014)
Rosmarinus off. (M)[RC2]	rosemary	calcareous soil	6.7	MTs, SQTs	ψ, $SWC_\%$	no	pots, greenhouse?	Ormeño et al. (2007)
Quercus ilex (M)[RC2]	oak	Silty clay loam	13.6	different MTs	ψ	yes	ambient	Lavoir et al. (2009)
Quercus robur (M, T)[RC2]	oak	70%, 30%	4.7	MTs, SQTs, selected OVOCs	$SWA_\%$	no	greenhouse	Boursoukidis et al. (2014)
Quercus virginiana Mill. (M)[RC2]	live oak	CPS: 100% org.?	5.0	Isoprene	SWC_v, ψ_{PD}	no	phytotron	Pegoraro et al. (2004b)

CPS: commercial potting soil (e.g. by Agrofino, Miracle Grow) including or plus fertilizer (Basacot), (A): arctic, (M): Mediterranean, (T): temperate

Table 3. Change for individual mono- and sesquiterpene species emission fluxes of *Fagus sylvatica* for two *SM* conditions (Rombach, 2018). Because of not normal distributed data, values are stated as median and 25th (lower) and 75th (upper) percentiles.

Species	$SWA_\%$		Total amount [μ g g(dw)$^{-1}$ h^{-1}]		Rel. amount [%]	
	A	B	A	B	A	B
monoterpenes	$\mathbf{6_4^8}$	$\mathbf{3_1^5}$	$\mathbf{11.7_{2.8}^{35.7}}$	$\mathbf{0.8_{0.4}^{2.4}}$	***100***	
sabinene	6_4^8	3_1^5	$11.2_{2.6}^{21.9}$	$0.2_{0.1}^{3.0}$	91_{79}^{95}	37_{23}^{75}
limonene	6_4^8	3_1^5	$0.3_{0.1}^{1.5}$	$0.1_{0.1}^{0.3}$	5_3^9	12_8^{19}
trans-β-ocimene	6_4^8	3_1^5	$0.2_{0.0}^{1.2}$	$0.2_{0.1}^{0.9}$	1_0^{10}	39_{10}^{64}
sesquiterpenes	$\mathbf{6_4^8}$	$\mathbf{3_1^5}$	$\mathbf{10.43_{2.88}^{17.23}}$	$\mathbf{27.65_{12.12}^{42.27}}$	***100***	
isolongifolene	6_4^8	3_1^5	$9.10_{2.22}^{15.57}$	$12.43_{6.60}^{30.17}$	88_{63}^{97}	82_{35}^{97}
longifolene	6_4^8	3_1^5	$0.39_{0.15}^{0.79}$	$0.30_{0.20}^{1.56}$	4_2^{12}	1_1^6
α-farnesene	6_4^8	3_1^5	$0.34_{0.05}^{0.57}$	$2.64_{0.21}^{6.56}$	3_1^7	9_1^{49}
junipene	6_4^8	3_1^5	$0.12_{0.04}^{0.15}$	$0.06_{0.04}^{0.50}$	1_1^2	1_0^6
α-bergamotene	6_4^8	3_1^5	$0.05_{0.02}^{0.07}$	$0.29_{0.05}^{0.77}$	0_0^1	1_0^6